Comparing Soil Dynamic Models for the Estimation of Reaction Forces on a Virtual Excavator Bucket

Eran Beeri Bamani[1], Solmon Jeong[1,2], Trevor Smith[1], and Hermano Igo Krebs[1]

***Abstract*— Virtual excavation requires credible soil–tool reaction forces for machine loading, control, and operator training. We compare the discrete element method (DEM), smoothed particle hydrodynamics (SPH), and extended position-based dynamics (XPBD) through matched replay of four dig–lift–dump bouts from one continuous acquisition. Each bout was independently replayed from the same initialized soil state using measured boom, arm, and bucket joint trajectories. Solver-specific reaction-force estimates were compared with a pressure-derived apparent wrench using common time alignment and coordinate conventions. XPBD achieved the lowest mean per-bout axis-averaged RMSE of 12.01 kN, reducing error by 40.5% relative to SPH and 67.9% relative to DEM. Because the reference was indirect and all bouts originated from one acquisition, the results establish a controlled within-acquisition ranking rather than general superiority. Independent trajectories, soil conditions, and direct force measurements are needed to assess generalization.**

I. Introduction

Virtual excavation requires both plausible soil motion and credible soil–tool reaction forces. These forces determine simulated machine loading and provide signals for feedback control, operator-facing force cues, and simulation-based development. A model may therefore produce visually plausible terrain motion while still giving misleading interaction dynamics. Force estimation is particularly difficult in excavation because it combines frictional contact, soil failure, large deformation, changing free surfaces, and material transport [1]. A practical simulator must balance force fidelity, numerical robustness, and computational tractability.

The discrete element method (DEM) represents soil as interacting particles governed by contact laws [2]. DEM studies using blades and excavator buckets have evaluated cutting forces, bucket filling, and soil motion [3], [4]. Smoothed particle hydrodynamics (SPH) reconstructs continuum fields from neighboring particles [5], allowing large deformation without a fixed mesh, and has been applied to cohesive and non-cohesive soil cutting [6]. Position-based dynamics (PBD) instead enforces constraints at the position level [7] and has been adapted for fast granular simulation [8]. Extended PBD (XPBD) introduces compliance and constraint-force estimates with reduced sensitivity to time step and solver iterations [9].

These formulations have generally been evaluated in separate experimental or numerical settings. Differences in tool geometry, prescribed motion, soil conditions, parameter selection, and force reference make the reported results

Fig. 1. Virtual excavator operator station used to acquire the joint trajectories evaluated through matched replay.

unsuitable for a controlled ranking across formulations. Prior DEM and SPH studies focused on method-specific physical cutting or bucket experiments, whereas related multiscale earthmoving work evaluated lower-resolution models primarily against a higher-resolution numerical reference [1]. An apparent difference between published results may therefore reflect the evaluation setting rather than the underlying soil–tool formulation.

A controlled comparison requires each formulation to experience the same tool motion and to be evaluated against the same force target. In this study, four dig–lift–dump bouts were replayed independently from the same initialized soil state using identical measured boom, arm, and bucket joint trajectories. This matched-replay design removes differences in commanded excavator motion while retaining common scoring windows, particle count, coordinate conventions, and time alignment. Hydraulic pressure and excavator kinematics provide a common apparent-wrench reference. Although indirect, this reference supplies a synchronized target for

TABLE I

Representative particle-based soil–tool simulation studies.

Study	Method / test case	Evaluation focus
Shmulevich et al. [3]	DEM / wide blade	Horizontal and vertical blade forces
Coetzee and Els [4]	DEM / bucket filling	Drag force, fill volume, and soil flow
Hu et al. [6]	SPH / soil cutting	Cutting force and soil deformation
Holz [8]	PBD / granular earthmoving	Stability and real-time performance
This work	DEM, SPH, XPBD / matched replay	Reaction-force agreement with a common reference

[1]Massachusetts Institute of Technology (MIT), Department of Mechanical Engineering, USA. Corresponding author: hikrebs@mit.edu.
[2]Sumitomo Heavy Industries, Ltd., Yokosuka, Kanagawa, Japan.

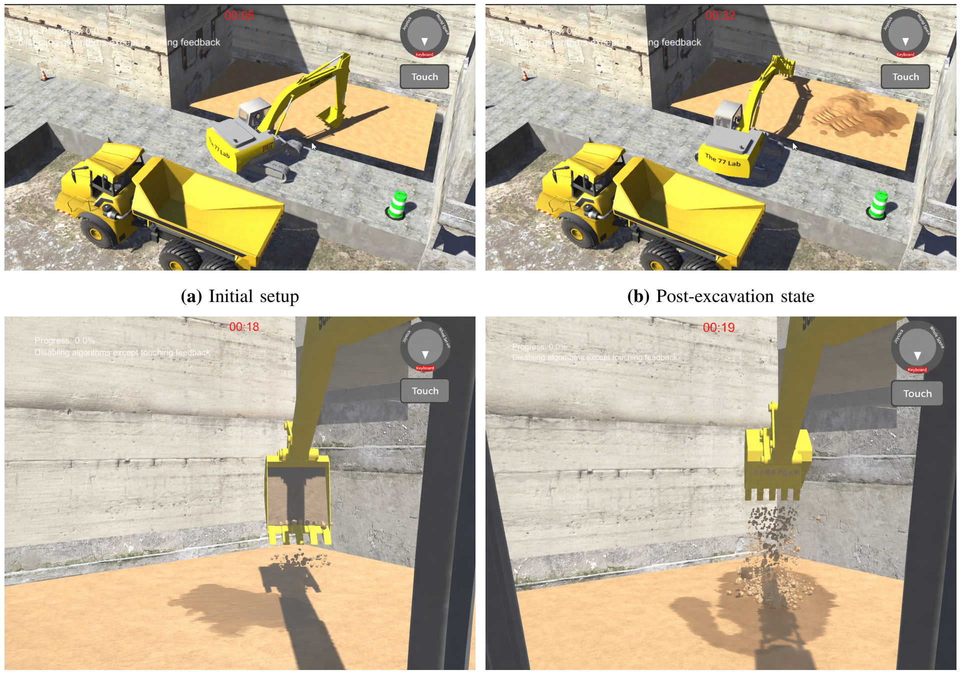

(a) Initial setup **(b)** Post-excavation state

(c) Material release **(d)** Granular discharge

Fig. 2. Representative SPH-based virtual excavation sequence used in the comparative study: (a) initial excavator and soil configuration, (b) deformation of the soil bed after excavation, (c) onset of material release from the bucket, and (d) subsequent granular discharge. The figure illustrates the simulated soil behavior; quantitative comparisons were based on the corresponding solver-specific reaction-force estimates.

within-acquisition comparison.

This work contributes (i) a matched-replay comparison of DEM, SPH, and XPBD; (ii) evaluation of their solver-specific reaction-force estimates against a common pressure-derived apparent wrench; and (iii) axis-wise and axis-averaged mean per-bout root-mean-square error (RMSE) across four excavation bouts. The resulting ranking is limited to the evaluated acquisition and indirect reference rather than interpreted as universal superiority.

II. Methodology

A. Soil–Tool Formulations

DEM, SPH, and XPBD represent soil deformation and tool interaction in different ways. DEM models soil as discrete particles governed by local normal and tangential contact laws [2]. SPH estimates continuum quantities from neighboring particles through a smoothing kernel, allowing large deformation without a fixed mesh [5]. XPBD represents the material through compliant positional constraints and iteratively projects the particle state toward constraint satisfaction [9].

For each formulation, the solver-native reaction-force estimate, including the constraint-force estimate where applicable, was resolved into the common evaluation frame as $\hat{F}_x(t)$ and $\hat{F}_z(t)$. A single fixed parameter set was used for each formulation across all four bouts, without bout-specific retuning. The formulation-specific parameter sets were inherited from the corresponding simulator implementations and were kept fixed throughout the evaluation.

The comparison treats each method as a complete end-to-end formulation. Constitutive assumptions, contact or constraint resolution, smoothing, numerical damping, and force recovery vary jointly among the formulations. The experiment therefore identifies the formulation with the lowest reference error under matched replay, but does not isolate the numerical mechanism responsible for the difference.

B. Virtual Environment and Evaluation Data

The virtual excavation environment was implemented in Unity 2019.4.1f1. Each formulation used a soil bed represented by 12,288 particles. Four dig–lift–dump bouts were segmented from one continuous excavator acquisition. Each bout was replayed independently from the same initialized soil state using the measured boom, arm, and bucket joint-angle trajectories.

The evaluation intervals, initial scene geometry, particle count, and coordinate convention were held fixed for DEM, SPH, and XPBD. The analysis considered the horizontal and vertical components of the bucket reaction, denoted by F_x and F_z and reported in kN. Figure 2 illustrates representative excavation and material-discharge states in the SPH environment.

The evaluation target was a pressure-derived apparent wrench reconstructed from hydraulic signals and excavator kinematics. Because this wrench was inferred rather than measured directly at the bucket–soil interface, it was treated as an indirect reference rather than contact-force ground truth. The same retained timestamps, time-alignment procedure, and coordinate/sign transformation were applied to all three model outputs.

C. Reference Construction and Bout Selection

The source acquisition provided paired head- and rod-side hydraulic-pressure channels for the boom, arm, and

TABLE II

REPLAY AND SCORING WINDOWS FROM THE 100-HZ ACQUISITION.

	Replay (s)		**Score (s)**		
Bout	**Start**	**End**	**Start**	**End**	N_b
1	22.99	29.91	23.89	29.91	603
2	39.79	46.56	40.69	46.56	588
3	56.63	63.14	57.53	63.14	562
4	73.00	79.52	73.90	79.52	563

bucket cylinders, together with linkage angles, at 100 Hz. Net cylinder forces and the corresponding generalized linkage moments were reconstructed from these signals. Using the measured angles and link lengths $(L_1, L_2, L_3) = (5.700, 2.941, 1.450)$ m, the generalized moments were mapped through planar inverse statics to an apparent bucket-tip wrench:

$$\mathbf{w}^{\text{ref}}(t) = \mathbf{G}(\boldsymbol{\theta}(t))^{-1}\,\mathbf{e}(t), \qquad \mathbf{w}^{\text{ref}}(t) = \left[F_x^{\text{ref}}(t), F_z^{\text{ref}}(t), M_f^{\text{ref}}(t)\right]^{\mathsf{T}}. \tag{1}$$

Here, $\mathbf{e}(t)$ contains the pressure-derived generalized moments, and $\mathbf{G}(\boldsymbol{\theta}(t))$ maps a bucket-tip wrench to those moments for the measured linkage configuration. Only F_x^{ref} and F_z^{ref} were retained because the soil–tool formulations estimate reaction-force components at the bucket tip but not the corresponding moment.

The reference reconstruction was cross-checked against an independent implementation, which reproduced the cylinder-force and bucket-tip-position channels to numerical precision. This check establishes consistency of the processing path but does not independently validate the physical wrench. The reference is therefore treated as an apparent wrench throughout the paper.

The reconstructed-force record was restricted to the verified 5.00–87.00 s portion of the acquisition because a kinematic discontinuity occurred after 87.00 s. All evaluated bouts ended by 79.52 s and were unaffected by this exclusion. Each replay included 0.90 s of leading context that was omitted from error accumulation identically for all formulations. The four non-overlapping scored windows contained 2,316 timestamps in total (Table II).

D. Evaluation Metrics

Let $m \in \{\text{DEM}, \text{SPH}, \text{XPBD}\}$ denote a formulation, b an excavation bout, $q \in \{x, z\}$ a force axis, and N_b the number of retained samples in bout b. The bout-wise force error was first computed as

$$E_{q,b}^{(m)} = \left[\frac{1}{N_b}\sum_{i=1}^{N_b}\left(\hat{F}_{q,b,i}^{(m)} - F_{q,b,i}^{\text{ref}}\right)^2\right]^{1/2}, \tag{2a}$$

$$\text{RMSE}_q^{(m)} = \frac{1}{B}\sum_{b=1}^{B} E_{q,b}^{(m)}, \tag{2b}$$

$$\text{RMSE}_{\text{axis}}^{(m)} = \frac{\text{RMSE}_x^{(m)} + \text{RMSE}_z^{(m)}}{2}, \qquad B = 4. \tag{2c}$$

TABLE III

MEAN PER-BOUT FORCE ERRORS ACROSS FOUR MATCHED BOUTS. VALUES ARE RMSE IN kN, WITH rRMSE (%) IN PARENTHESES.

Quantity	F_x	F_z	**Axis avg.**
Apparent ref. RMS (kN)	55.25	27.33	–
DEM	40.39 (73.1%)	34.51 (126.3%)	37.45 (99.7%)
SPH	19.39 (35.1%)	21.00 (76.8%)	20.20 (56.0%)
XPBD	**9.65 (17.4%)**	**14.37 (53.6%)**	**12.01 (35.5%)**

Equation (2a) defines the RMSE within each bout, Eq. (2b) gives the equally weighted mean across the four bouts, and Eq. (2c) gives the component-wise axis average.

Relative RMSE was computed using the RMS amplitude of the corresponding apparent-reference force component:

$$S_{q,b}^{\text{ref}} = \left[\frac{1}{N_b}\sum_{i=1}^{N_b}\left(F_{q,b,i}^{\text{ref}}\right)^2\right]^{1/2}, \tag{3a}$$

$$\text{rRMSE}_q^{(m)} = \frac{100}{B}\sum_{b=1}^{B}\frac{E_{q,b}^{(m)}}{S_{q,b}^{\text{ref}}}, \tag{3b}$$

$$\text{rRMSE}_{\text{axis}}^{(m)} = \frac{\text{rRMSE}_x^{(m)} + \text{rRMSE}_z^{(m)}}{2}. \tag{3c}$$

Table III reports the mean bout-wise reference RMS amplitude, defined as

$$\bar{S}_q^{\text{ref}} = \frac{1}{B}\sum_{b=1}^{B} S_{q,b}^{\text{ref}}. \tag{4}$$

Pointwise percentage error was avoided because division by small or zero-crossing signed reference forces can produce ill-conditioned values. Accordingly, rRMSE expresses error relative to the apparent reference rather than physical soil-contact percent accuracy.

Bout-wise aggregation gives each bout a weight of $1/4$ despite their slightly different sample counts. The axis average similarly gives equal weight to F_x and F_z and is not a vector RMSE. The 2,316 timestamps were not treated as independent experimental replications.

III. RESULTS

Figure 2 provides qualitative context for soil-bed deformation and material discharge. The quantitative comparison is based on the matched-bout errors reported in Table III.

XPBD produced the lowest mean per-bout RMSE on both evaluated axes, with 9.65 kN for F_x and 14.37 kN for F_z. SPH yielded 19.39 and 21.00 kN, respectively, whereas DEM yielded 40.39 and 34.51 kN. The corresponding axis-averaged RMSE values were 12.01 kN for XPBD, 20.20 kN for SPH, and 37.45 kN for DEM.

XPBD reduced the axis-averaged RMSE by 67.9% relative to DEM and 40.5% relative to SPH. Its lower axis average did not mask degradation on either component, because XPBD ranked first independently for both F_x and F_z.

The XPBD axis-averaged RMSE values for Bouts 1–4 were 13.26, 13.38, 10.96, and 10.42 kN, respectively. Their 2.96-kN range indicates that the aggregate result was not determined by one exceptionally favorable bout. Because all four bouts originated from one continuous acquisition, this variation is reported descriptively rather than as independent experimental replication. XPBD's aggregate F_z error remained 4.72 kN higher than its F_x error, identifying the vertical component as the clearer target for further improvement. The present experiment cannot determine whether this larger residual originates primarily from the vertical soil-response model or from uncertainty in the pressure-derived reference reconstruction.

IV. Discussion and Conclusion

A. Interpretation and Relevance

Under matched replay, XPBD showed the closest agreement with the pressure-derived apparent wrench on both evaluated force axes, while SPH was intermediate and DEM produced the largest errors. Because the same joint trajectories, scoring windows, initialized soil state, particle budget, coordinate convention, and reference were used for all formulations, the ranking is not attributable to differences in commanded excavator motion or evaluation conditions. XPBD ranked first independently for both F_x and F_z, so its lower axis-averaged error does not mask degradation on either component.

Beyond the resulting ranking, matched replay removes motion-level feedback by prescribing the same measured joint trajectories. This isolates reaction-force differences along a common kinematic path and provides a practical first-stage screen before closed-loop, runtime, or operator evaluations.

The comparison treats DEM, SPH, and XPBD as complete end-to-end formulations. Their constitutive assumptions, contact or constraint resolution, numerical damping, and force-recovery procedures differ jointly. The present results therefore do not identify which individual XPBD feature caused the lower error; that question would require controlled solver ablations.

Lower force-reference error makes XPBD the strongest candidate among the three evaluated formulations for continued virtual-excavation development. Such force estimates may support controller evaluation, operator-facing force cues, and simulation-based policy development. However, this offline comparison does not establish real-time solver performance, closed-loop haptic stability, or sim-to-real transfer.

B. Limitations and Future Validation

The four bouts came from one continuous acquisition and were replayed from a common initialized soil state; thus, they neither provide independent tests across soil types, trajectories, machines, or operating conditions nor preserve soil-history effects between successive digs. In addition, the reference wrench was reconstructed from hydraulic pressure and planar kinematics rather than measured directly at the bucket–soil interface. It may contain errors associated with pressure calibration, linkage geometry, unmodeled dynamics, friction, and load compensation.

RMSE summarizes overall force disagreement but does not separately describe peak error, phase lag, impulse, mechanical work, or unloading transients. A common particle count also does not guarantee equal effective resolution across the three formulations, and runtime was not benchmarked under matched conditions.

Future validation should use independent acquisitions spanning different soils, bucket velocities, penetration depths, and dig geometries. Direct multi-axis force measurement at the bucket would help separate model error from reference-reconstruction error. Force fidelity should also be evaluated together with transient metrics and matched runtime measurements before closed-loop haptic or autonomous excavation tests.

C. Conclusion

Within the evaluated acquisition, XPBD achieved the lowest mean per-bout RMSE on both force axes, with an axis-averaged error of 12.01 kN compared with 20.20 kN for SPH and 37.45 kN for DEM. The matched-replay protocol supports a controlled within-acquisition ranking and identifies XPBD as the preferred formulation for continued validation. The indirect reference, single acquisition, RMSE-based evaluation, and absence of a matched runtime benchmark prevent interpreting the result as universal superiority.

Acknowledgment

This work was supported by Sumitomo Heavy Industries, Ltd. (Grant No. 6941094), and by institutional funding from the Massachusetts Institute of Technology. The study protocol was reviewed and deemed exempt by the MIT Committee on the Use of Humans as Experimental Subjects (COUHES; Protocol E-3460) under Exempt Category #3, Benign Behavioral Intervention.

References

[1] M. Servin, T. Berglund, and S. Nystedt, "A multiscale model of terrain dynamics for real-time earthmoving simulation," *Advanced Modeling and Simulation in Engineering Sciences*, vol. 8, no. 1, p. 11, 2021.

[2] P. A. Cundall and O. D. L. Strack, "A discrete numerical model for granular assemblies," *Géotechnique*, vol. 29, no. 1, pp. 47–65, 1979.

[3] I. Shmulevich, Z. Asaf, and D. Rubinstein, "Interaction between soil and a wide cutting blade using the discrete element method," *Soil and Tillage Research*, vol. 97, no. 1, pp. 37–50, 2007.

[4] C. J. Coetzee and D. N. J. Els, "The numerical modelling of excavator bucket filling using DEM," *Journal of Terramechanics*, vol. 46, no. 5, pp. 217–227, 2009.

[5] R. A. Gingold and J. J. Monaghan, "Smoothed particle hydrodynamics: Theory and application to non-spherical stars," *Monthly Notices of the Royal Astronomical Society*, vol. 181, no. 3, pp. 375–389, 1977.

[6] M. Hu, T. Gao, X. Dong, Q. Tan, C. Yi, F. Wu, and A. Bao, "Simulation of soil–tool interaction using smoothed particle hydrodynamics (SPH)," *Soil and Tillage Research*, vol. 229, p. 105671, 2023.

[7] M. Müller, B. Heidelberger, M. Hennix, and J. Ratcliff, "Position based dynamics," *Journal of Visual Communication and Image Representation*, vol. 18, no. 2, pp. 109–118, 2007.

[8] D. Holz, "Parallel particles (P2): A parallel position based approach for fast and stable simulation of granular materials," in *Workshop on Virtual Reality Interaction and Physical Simulation*, pp. 135–144, The Eurographics Association, 2014.

[9] M. Macklin, M. Müller, and N. Chentanez, "XPBD: Position-based simulation of compliant constrained dynamics," in *Proceedings of the 9th International Conference on Motion in Games*, pp. 49–54, Association for Computing Machinery, 2016.